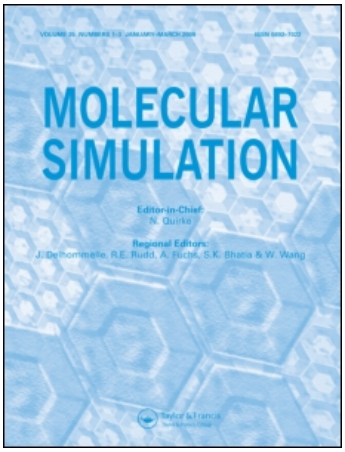

Molecular Simulation
Publication details, including instructions for authors and subscription information:
http://www.informaworld.com/smpp/title~content=t713644482

Molecular Dynamics Simulations on Aqueous Solutions of Rare Gases

Hideki Tanaka[a]; Koichiro Nakanishi[a]
[a] Department of Industrial Chemistry, Kyoto University, Kyoto, Japan

To cite this Article Tanaka, Hideki and Nakanishi, Koichiro(1991) 'Molecular Dynamics Simulations on Aqueous Solutions of Rare Gases', Molecular Simulation, 6: 4, 311 — 324
To link to this Article: DOI: 10.1080/08927029108022439
URL: http://dx.doi.org/10.1080/08927029108022439

Molecular Simulation, 1991, Vol. 6, pp. 311–324
Reprints available directly from the publisher
Photocopying permitted by license only

MOLECULAR DYNAMICS SIMULATIONS ON AQUEOUS SOLUTIONS OF RARE GASES

HIDEKI TANAKA and KOICHIRO NAKANISHI

Department of Industrial Chemistry, Kyoto University, Sakyo, Kyoto, 606, Japan

(*Received May 1990, accepted August 1990*)

Molecular dynamics simulations for water and aqueous solutions of apolar rare gases have been carried out in order to study the dependence of hydration structures on solute species. The solute species under investigation were neon and xenon. The structures and thermodynamic properties relevant to the hydration processes were analyzed based upon the quenching of the system to local potential energy minima. It was found that the two solutes give rise to qualitatively different hydration structures; the introduction of Xe atoms make a significant water-structure enhancement, increasing the population of pentagonal hydrogen bond network. The solution of neon with usual size parameter and combining rule failed to reproduce the experimentally observed properties. The structural change in quenched state was seen in the Ne solution where a somewhat larger size parameter was adopted. In normal mode analysis, the potential energy was expanded up to quadratic order around quenched configurations. Free energy and entropy changes in the hydration were evaluated for these aqueous harmonic systems. It was shown that a substantial part of the negative entropy change in hydration of apolar molecules experimentally observed arises from the differences in molecular rearrangement and anharmonic rather than harmonic motions.

KEY WORDS: Molecular dynamics, aqueous solution, hydrophobic hydration, rare gas.

I. INTRODUCTION

Water and aqueous solutions are major subjects in the field of solution chemistry. Liquid water exhibits several anomalous thermodynamic properties in the ambient temperature and pressure range [1]. These anomalies might be originated from the hydrogen bond network existing even in liquid state, although the network in liquid state may be quite different from that in ice. Hydrogen bonded clusters which are considered to be solid like are more bulky than water monomers which do not participate in hydrogen bond network. The number of water molecules engaged in this network tends to decrease with increasing temperature. Thus, the existence of the hydrogen bond network is responsible for the appearance of minimum at 4°C and 1 atm in the temperature dependence of the molar volume. Other thermodynamic quantities are explained likewise. Although this interpretation should not be accepted literally, it involves some insight into the microscopic nature of liquid water.

Hydrogen bonds in water seem to play a further important role in the hydration of hydrophobic solutes. The hydration is characterized by thermodynamic excess functions; large negative entropy, negative enthalpy, and the resultant positive free energy [2]. The large negative entropy change and exothermic hydration process is usually accounted for on the basis of a structure enhancement of water around a solute, which is referred to as hydrophobic hydration. The idea of the structure enhancement is undoubtedly deduced from the stability of clathrate hydrates. None of the known

clathrate structures, however, coincides with ice structure. It is dependent on guest molecular species. Furthermore, the similarity between clathrate hydrates and aqueous solutions of apolar solutes is far from clear in view of the temperature and the solute concentration at which both systems are stable.

The solubility of simple and spherical solutes into water has the following trends with solute species [2]. The larger the solute size becomes, the higher the solubility becomes: Xe is more soluble than Ne. Both the enthalpic and entropic terms (excess entropy times temperature) in Xe solution are more negative than those in Ne solution. However, the entropy term is relatively less dominant in Xe solution. The hydration mechanism of even spherical molecules is fairly complicated. These thermodynamic properties have microscopically two origins: one is the cavity formation of corresponding size in water to accommodate the solute and the other is the interaction between water and solute. The structural effect is closely related to the cavity formation. Since the free energy for the cavity formation is likely to be dependent on the cavity size, it is difficult to explain why these solubilities are experimentally observed only on the basis of simple and traditonal structural-effect of water around a solute. It is therefore desirable to show how the water structure adjacent to a solute depends on the solute size.

There are several studies focusing on the solubility of simple hydrophobic solutes into water and structures around them [3–7]. Swope and Andersen [4] discussed the temperature dependence of the solubility and pointed out that it is impossible to reproduce an observed solubility versus temperature curve without introducing an unusual combining rule: enlarge the neon diameter to more than 3 Å from a measured value 2.8 Å. Apart from the physical origin of this combining rule, which may arise from three and higher body interactions, it is highly desirable to examine the effect of solute size on hydration structure.

So called quenching to local energy minimum structure [8] seems to be a convenient way to investigate structures of liquids and solutions. This method has been applied to water cluster [9] and water [10], where the continuous trajectory of water molecules can be divided into a discrete set of configurations. The quenched structures do not suffer from complicated thermal motions and involve purely structural information. Thus, hydrogen bond network analysis in quenched structures has an essential meaning. The potential energy is expanded at each quenched structure up to quadratic order for small displacements from quenched structures. This leads to normal mode analysis, which corresponds to the enumeration of vibrational density of state. Free energy and entropy changes are estimated within a harmonic approximation making use of the density of state. The solute molecules may significantly perturb several modes, from which we are able to discuss the relation between free energy change and solute size. In the following sections, we will present the methods and results of molecular dynamics(MD) simulation and quenching, normal mode analysis.

II. MODELS AND METHODS

Conventional MD simulations (NEV ensemble) with periodic boundary condition have been carried out for pure water and aqueous solutions of rare gases. An MD simulation for pure water was used as a standard system, for comparison with each aqueous solution. The solute species under investigation are neon (Ne) and xenon

Table 1 Lennard-Jones parameters for Ne, Nr, and Xe. Lorentz-Berthelot rule is adopted for a solute and water pair

solute	σ (Å)	ε (kJ/mol)
Ne	2.749	0.2958
Nr	3.100	0.7531
Xe	4.100	1.8030

(Xe) since the observed thermodynamic excess functions are fairly different from each other as mentioned.

a. Potential Model

We adopted the TIP4P potential [11] in describing intermolecular interactions for the water dimer because it is well known that this potential succeeds in reproducing both static and dynamic properties of water in its pure state. A slight modification was applied to the original potential by multiplying a switching function which truncates the interaction smoothly in order to perform the quenching and normal mode analysis efficiently. The multiplication of this type of switching function does not influence the short range order [12]. The functional form is given elsewhere [10]. This also served to avoid taking a lattice sum which makes a simulation costly.

The interactions between solute and water (oxygen atom) and between solutes were approximated by Lennard-Jones (LJ) potentials. The potential parameters between solutes [13] are given in Table 1. The interaction between water and solute was described by a usual Lorentz-Berthelot rule, where the LJ parameters of oxygen on water molecule were set to those identical to parameters for Ne. According to Swope and Andersen's findings concerning to the solubility of Ne, the present study was supplemented by an additional simulation where a size parameter for Ne was slightly enlarged as given in Table 1 (hereafter referred to as Nr).

b. MD Simulation

In the pure system, experimental density at 1 atm and at 298.15 K was adopted [1]. The number of molecules was 216 including solutes (in the cases of solution). In the present simulations, any solution whose solute concentration is 3 mol%, exceeds the solubility limit and may be somewhat artificial. This choice is, however, inevitable because the hydration properties both in MD generated and quenched configurations must be calculated with certain precision.

At initial stage of MD simulation, velocities and angular velocities were adjusted so that the temperature of the system could correspond to 298.15 K. The simulations were extended to 75,000 time steps for Ne and Xe, 50,000 for Nr, and 25,000 for water with time step of $\Delta t = 4.0 \times 10^{-16}$. The last 25,000 steps of each solution and 10,000 steps of pure water were used for the calculation of thermodynamic and structural properties.

c. Quenching

The quenching of the system corresponds to the mapping of MD generated configurations onto their potential energy local minimum configurations. This procedure is

performed by solving partial differential equation as

$$dx/dt = -\partial V/\partial x, \tag{1}$$

where V stands for the potential energy of the system and x denotes six coordinates of each molecule; three center of mass coordinates and three Euler angles to specify molecular orientation. The quenching was executed effectively by small amounts of displacements in molecular coordinates, which are proportional to the gradient of the potential energy at each quenching step. Further complicated algorithm such as predictor-corrector method in solving the equation (1) is found to be unnecessary in the present calculation. The CPU time required for obtaining one quenched configuration starting from an MD generated configuration corresponds to that for an ordinary MD simulation of 20,000 to 40,000 steps. It is obvious that the evaluation of the gradient of potential with respect to Euler angles demands more CPU time than with respect to center of mass coordinates. If torques assessed simply from forces acting on each interaction site can be transformed into the derivatives of the potential energy with respect to Euler angles, it is of great advantage to practical quenching. The relation between two kinds of generalized forces is established intuitively, or by equating the second time derivatives of Euler angles appearing in both Lagrange and Euler equations of motion as

$$\begin{aligned} \partial V/\partial\theta &= N_X\cos\psi - N_Y\sin\psi \\ \partial V/\partial\phi &= N_X\sin\theta\sin\psi + N_Y\sin\theta\cos\psi + N_Z\cos\theta \\ \partial V/\partial\psi &= N_Z, \end{aligned} \tag{2}$$

where Euler angles ($\theta\,\phi\,\psi$) are defined in usual manner [14] and N is the torque acting on each molecule in the molecule-fixed framework.

The quenched structures of 80 configurations each separated by 50 f.s. for pure water and 100 configurations separated by 100 f.s. for solutions were obtained. The quench process obtaining one configuration required 20 to 30 min. using HITAC S820 supercomputer when the derivatives of the potential energy with respect to Euler angles are evaluated directly. Adopting a neighbor list and a transformation of the torque to the Euler angle derivatives of potential could facilitate the quenching process and resulted in 5 to 7 min. to obtain one quenched configuration. The neighbor list method coded for supercomputer worked quite effectively because the list need not be renewed frequently as the quenching proceeded.

d. Normal Mode Analysis

Normal mode analyses were designed to evaluate free energies and entropies of the systems. The analyses were performed by the diagonalization of the mass weighted force constant matrix. In the present case, the second derivatives of the potential were analytically expressed. The detailed method is given by Pohorille *et al.* [15]. In actual process for normal mode analysis, a problem concerning to the kinetic energy tensor, which is expressed in terms of Euler angles, arises: one of the eigen values of the kinetic tensor becomes zero, if θ approaches 0 or π. This difficulty originating in our numerical treatment can be circumvented by adopting alternative definitions of Euler angles.

Table 2 Thermodynamic properties for pure water (W) and aqueous solutions of Ne, Nr, and Xe. All the units are in kJ/mol except for the temperature (K). * denotes corrected value where the system corresponds to standard state with respect to temperature, 298.15K, H, U, Uw, S, G, and T are enthalpy, energy of the system, energy of water, entropy, Gibbs free energy, and temperature of the system, respectively. Δ means hydration property, and E denotes excess quantity.

System	W	Ne	Nr	Xe
		experimental		
ΔH^E		−7.66		−17.95
$T\Delta S^E$		−35.93		−41.91
ΔG^E		28.24		23.93
		MD simulation		
T	301.0	295.3	300.4	293.5
U	−42.07	−40.92	−40.76	−41.39
ΔH^E		+7.6	+14.4	−12.6
ΔH^{E*}		+16.9	+13.2	+0.4
Uw^*	−42.21	−41.74	−41.80	−42.03
		quenched configuration		
U	−52.24	−50.81	−50.82	−51.00
ΔU^E		+9.2	+8.8	+0.9
Uw	−52.24	−51.98	−51.96	−52.05

III. RESULTS AND DISCUSSION

a. Static Properties in MD Generated Structure

The thermodynamic properties directly obtained from the present MD simulations are listed in Table 2. The hydration properties are also shown after corrections of the

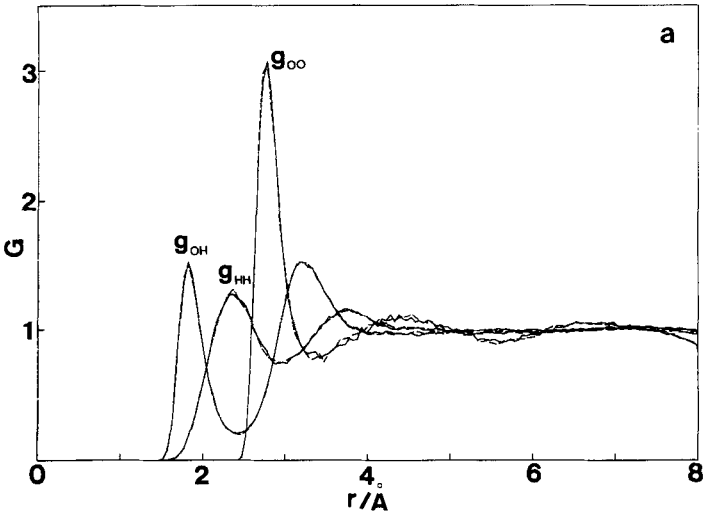

Figure 1 Site-site radial distribution functions for water and aqueous solutions obtained from MD generated configurations. (a): Ne, (b): Nr, (c): Xe solutions; solid line: RDF in aqueous solution, dashed line: RDF in pure water.

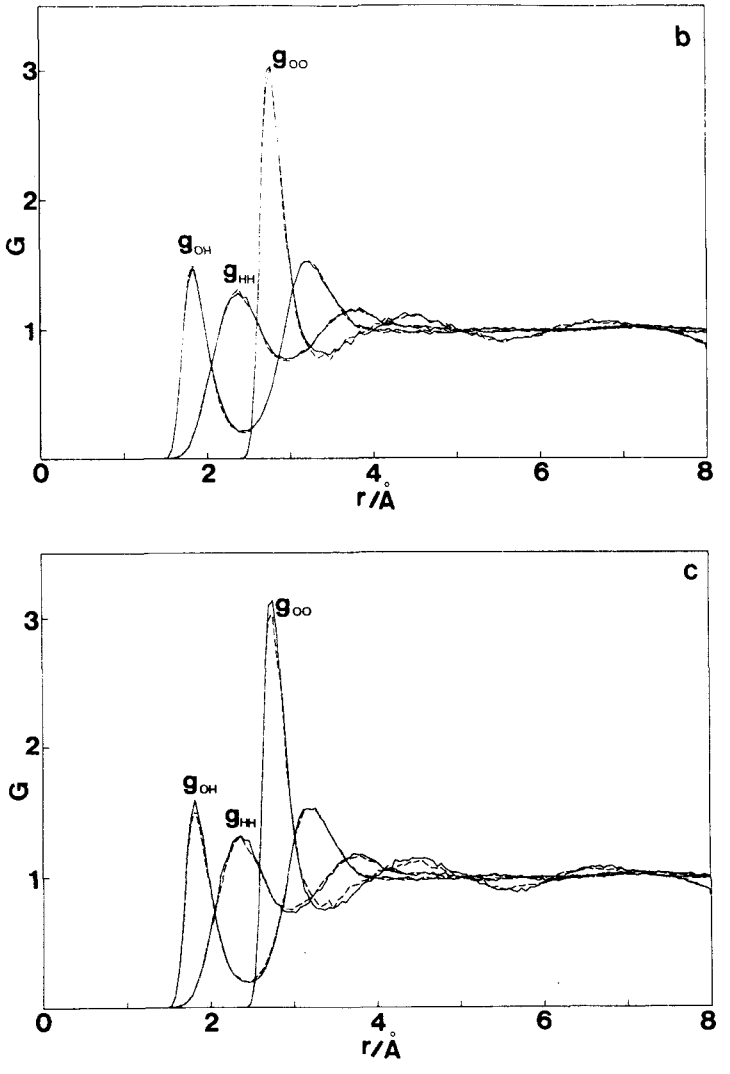

Figure 1 *(Continued)*

potential energies due to the drifting the temperature and due to the additional pV term (p; pressure, V: volume of the system) in the hydration (p is assumed to be 1 atm). The heat capacity required for the correction was set tentatively to experimental value of pure water 74 kJ mol^{-1} K^{-1} [1]. We will restrict ourselves to discussion on the corrected "enthalpies" only.

In each solution, an excess enthalpy from MD simulation is positive and does not agree with the experimental one at infinite dilution. The discrepancy seems to arise mainly from higher solute concentration in MD simulation. The introduction of single apolar atom into water should result in fairly large exothermic hydration, if potential models used in the simulation are correct. The negative hydration enthalpy

expected at infinite dilution may be cancelled at higher concentration by the existence of other apolar solutes, which make weak interaction with water. In fact, the preliminary Monte Carlo simulations show that the tendency of enthalpies versus solute species agree with experimental ones for infinitely dilute solutions of Nr and Xe[16]. At infinite dilution, the enthalpy exhibits too large a positive value only in the Ne solution.

The water structure in each solution is compared with that of pure water to account for the above energy difference. This comparison was materialized by site–site radial distribution functions (RDFs), which are shown in Figure 1. The differences in RDFs for water between pure water and Ne solution are very small as seen in Figure 1a. The RDFs in the Nr solution (Figure 1b) exhibit only slight structural change. On the other hand, a substantial change in the first peak of each site–site distribution function occurs by the existence of Xe atoms as can be seen from Figure 1c.

b. Static Properties in Quenched Structure

Thermodynamic excess functions calculated from quenched structures are also given in Table 2. Most of the energetic characteristics in quenched structure are similar to those in MD simulation. However, a comparison of these potential energy differences in MD generated and quenched structure is worth noting since it is possible to extract some information on the origin of the hydration energy differences for different species in Table 2. There are two candidates to account for the difference: one is the difference in the vibrational density of state including both harmonic and anharmonic contributions and the other is the difference in potential energy of quenched configurations. The former is closely related to the curvatures to which the system is quenched and is manifested in thermal effects. The latter is concerned with the effect due to water structure changes caused by the apolar molecules. In other words, while the potential energy in quenched structure is concerning to only mechanically stable configurations, the potential energy in MD generated structures involved information on wide range of potential surfaces; the vibrational density of state as well as quenched structures. We examined the potential energy differences of water in pure water and aqueous systems; $\Delta\ Uw = Uw$(solution) $- Uw$ (pure water) in Table 2 in order to estimate the relative magnitude of above two origins. In MD generated structures, the potential energy increases for Ne, Nr, Xe solutions are 0.47, 0.41, 0.18 kJ/mol, respectively. The corresponding values in quenched structures are 0.26, 0.28, 0.18 kJ/mol. The energy differences defined as $\Delta\Delta\ Uw = \Delta\ Uw$ (MD-generate) $- \Delta\ Uw$ (quenched) are 0.21, 0.13, 0 kJ/mol, respectively. These values have some meaning although they do not agree with the experimentally observed values due to the higher concentration as discussed above. The result indicates that the anharmonic contributions in Xe solution are almost same as in pure water and that anharmonic terms, which are significantly large in pure water, are less important in Ne (Nr) solution. This means that the introduction of Ne (Nr) solute makes some modes slightly harder compared with pure water, because the increase in potential energy difference for MD simulation is fairly larger than in quenched state and this must be due to the decrease in soft modes.

The RDFs for quenched pure water and solutions are shown in Figure 2. Since the systems are mechanically stable and free from thermal excitation, the RDFs show highly ordered packings. There exists no difference between RDFs for the Ne solution and for pure water in all distance ranges. The RDFs for oxygen pair in the Nr and

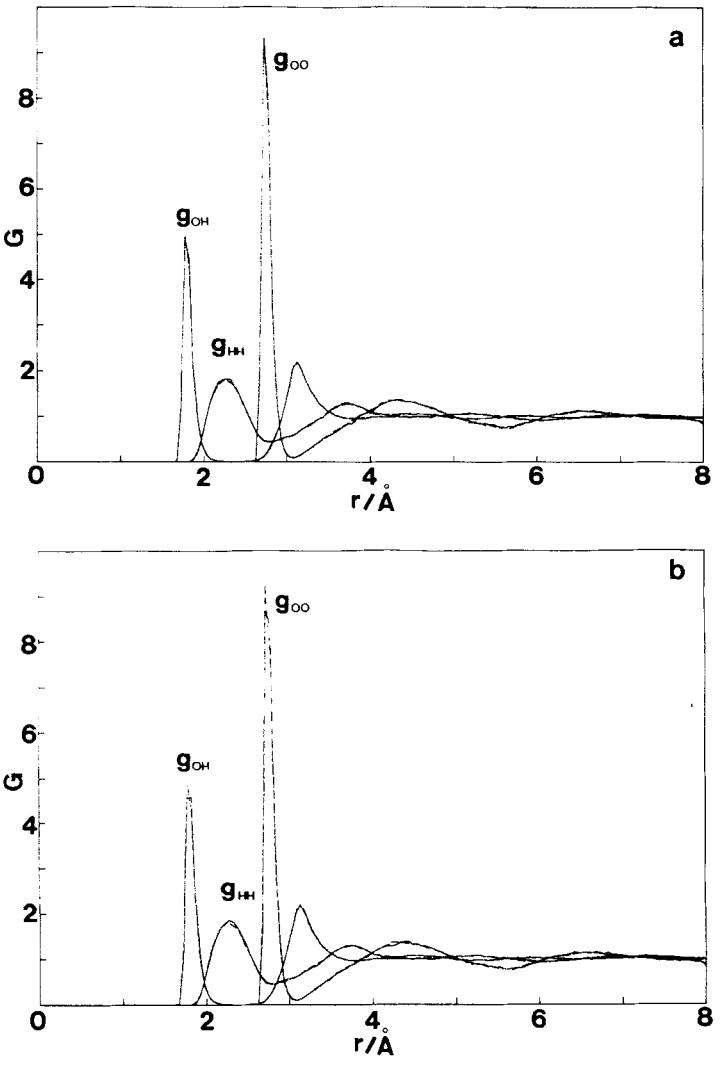

Figure 2 Site-site radial distribution functions for water and aqueous solutions obtained from quenched configuations. (a): Ne, (b): Nr, (c): Xe solutions; solid line: RDF in aqueous solution, dashed line: RDF in pure water.

Xe solutions are qualitatively different from that of pure water. The first peaks in both solutions shift to a longer distance as compared to pure water. To see the shifts more easily, those values at which the RDFs take maxima are given in Table 3. Further change in the height of the first peak can be observed in Xe solution. The structure analogous to clathrate hydrate may be constructed when a solute diameter becomes larger than 3 Å.

This structural change is also investigated by means of network analysis in which the rings formed by hydrogen bonds are counted. The definition of the hydrogen bond adopted in this analysis relies only on the pair potential energy. The average numbers

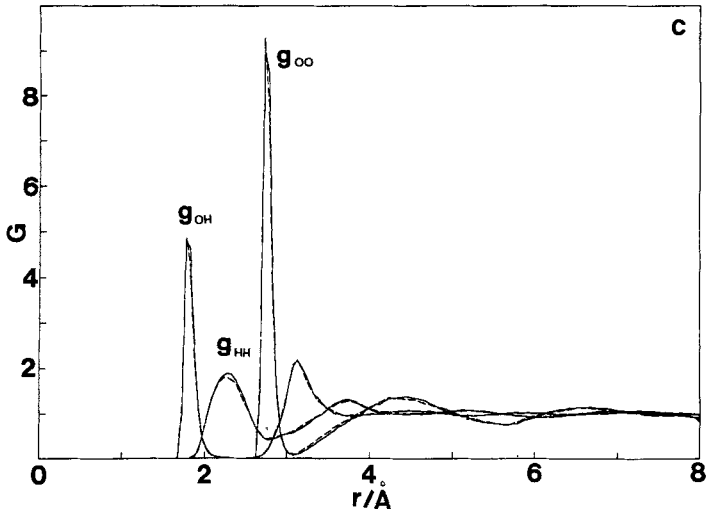

Figure 2 *(Continued)*

of each ring for various but reasonable hydrogen bond criteria are listed in Table 4. The ring numbers simply enumerated in the case of solutions are divided for comparison by the water mole fraction in the table because numbers of rings are expected to be linearly dependent on the number of water molecules. There is no typical characteristics in the ring number distribution based on MD generated structure. Whereas low pressure iceIh, which is already quenched, consists of only 6 membered rings for any threshold value given in the table, there exist several kinds of hydrogen-bonded rings ranging from 4 to 10 in quenched water from its liquid state. The distribution for solution is fairly different from that for pure water: the number of cyclic pentamer increases in quenched Xe solution. The several examples of quenched structure are given in Figure 3. It is easily seen that the hydrogen bond network in the quenched water is quite different from that in iceIh. Moreover, the increase in number of pentamers could be seen in the Xe solution.

Table 3 The height of first peak in site–site radial distribution functions for pure water and aqueous solutions. The distance at which each radial distribution function has the first peak is given in parenthesis(Å)

site–site system	OH*(1.78)*	OH*(1.83)*	OO*(2.73)*	OO*(2.78)*
		quenched		
Water	4.92	4.20	9.27	7.67
Ne	4.95	4.43	9.32	8.09
Nr	4.56	4.57	8.67	8.39
Xe	4.80	4.64	9.02	8.50
		MD generated		
Water	1.42	1.51	2.49	3.02
Ne	1.37	1.53	2.38	3.08
Nr	1.37	1.48	2.39	2.88
Xe	1.46	1.59	2.54	3.10

Table 4 Ring number distributions for quenched water and aqueous solutions and those for MD generated configurations. Hydrogen bond energy is in kJ/mol. The ring numbers are linearly scaled so that number of water molecules in solution is the same as in pure water

system	*energy*	*ring size* 3	4	5	6	7	8	9
				(quenched configuration)				
Water	−12	0.90	29.11	78.58	91.60	16.98	0.14	0.00
	−14	0.53	24.08	69.39	83.01	23.49	0.81	0.03
	−16	0.38	16.13	52.54	62.83	31.33	3.53	0.20
	−18	0.20	7.04	27.25	30.44	25.33	11.44	3.45
Ne	−12	1.15	28.77	79.36	93.9	16.12	0.13	0.00
	−14	0.59	24.29	69.88	84.14	21.51	0.69	0.00
	−16	0.44	16.53	52.74	64.36	29.10	3.63	0.25
	−18	0.20	8.13	28.25	33.68	23.88	9.09	2.99
Nr	−12	0.87	30.75	79.54	84.74	13.51	0.27	0.00
	−14	0.45	26.15	70.44	77.86	19.09	0.69	0.00
	−16	0.31	17.31	51.70	59.41	25.90	3.80	0.33
	−18	0.10	7.52	25.66	29.31	21.21	10.39	4.05
Xe	−12	1.47	31.90	78.74	85.64	14.06	0.11	0.00
	−14	0.90	27.60	70.81	80.42	19.34	0.46	0.01
	−16	0.63	18.88	55.20	64.54	26.82	2.54	0.20
	−18	0.36	8.72	30.39	34.70	25.21	8.63	2.62
				(MD generated configuration)				
Water	−12	0.96	10.23	23.41	24.56	18.99	9.34	3.95
	−14	0.25	5.08	12.35	12.29	9.71	6.91	5.86
	−16	0.11	2.11	5.03	4.03	3.19	2.76	2.49
	−18	0.05	0.68	1.30	0.84	0.40	0.35	0.35
Ne	−12	1.50	9.22	22.81	25.66	19.35	9.56	4.14
	−14	0.52	4.46	11.33	11.40	9.55	7.39	6.41
	−16	0.19	1.96	4.15	3.90	2.70	2.45	2.59
	−18	0.05	0.68	1.11	0.72	0.54	0.26	0.31
Nr	−12	1.13	9.45	22.07	22.90	17.30	9.11	3.51
	−14	0.32	4.56	11.56	10.23	8.05	6.46	4.86
	−16	0.10	1.76	4.11	3.41	2.27	1.98	2.00
	−18	0.01	0.52	0.90	0.55	0.27	0.20	0.27
Xe	−12	1.46	10.62	25.03	28.10	21.19	9.12	2.86
	−14	0.44	5.39	13.27	13.68	11.74	7.44	5.72
	−16	0.11	2.34	5.32	4.83	3.57	2.70	3.03
	−18	0.01	0.78	1.39	1.02	0.52	0.30	0.39

c. Normal Mode Analysis

The normal mode analysis using quenched structures was made and the density of states for molecular translation and rotation obtained are shown in Figure 4. The figure shows that the difference in normal mode is larger in low frequency region and higher frequency modes are hardly affected. This is because the high frequency modes above $350\,cm^{-1}$ correspond to almost exclusively rotational motions and the solute motion can couple with low frequency translational motions of water molecules. Free energies A' and entropies S' for the systems are evaluated within a harmonic approximation using normalized (to unity) density of state $g(\omega)$ as

$$A'/kT = \alpha \int \ln(\beta\hbar\omega)\, g(\omega)\, d\omega + U_q \qquad (3)$$

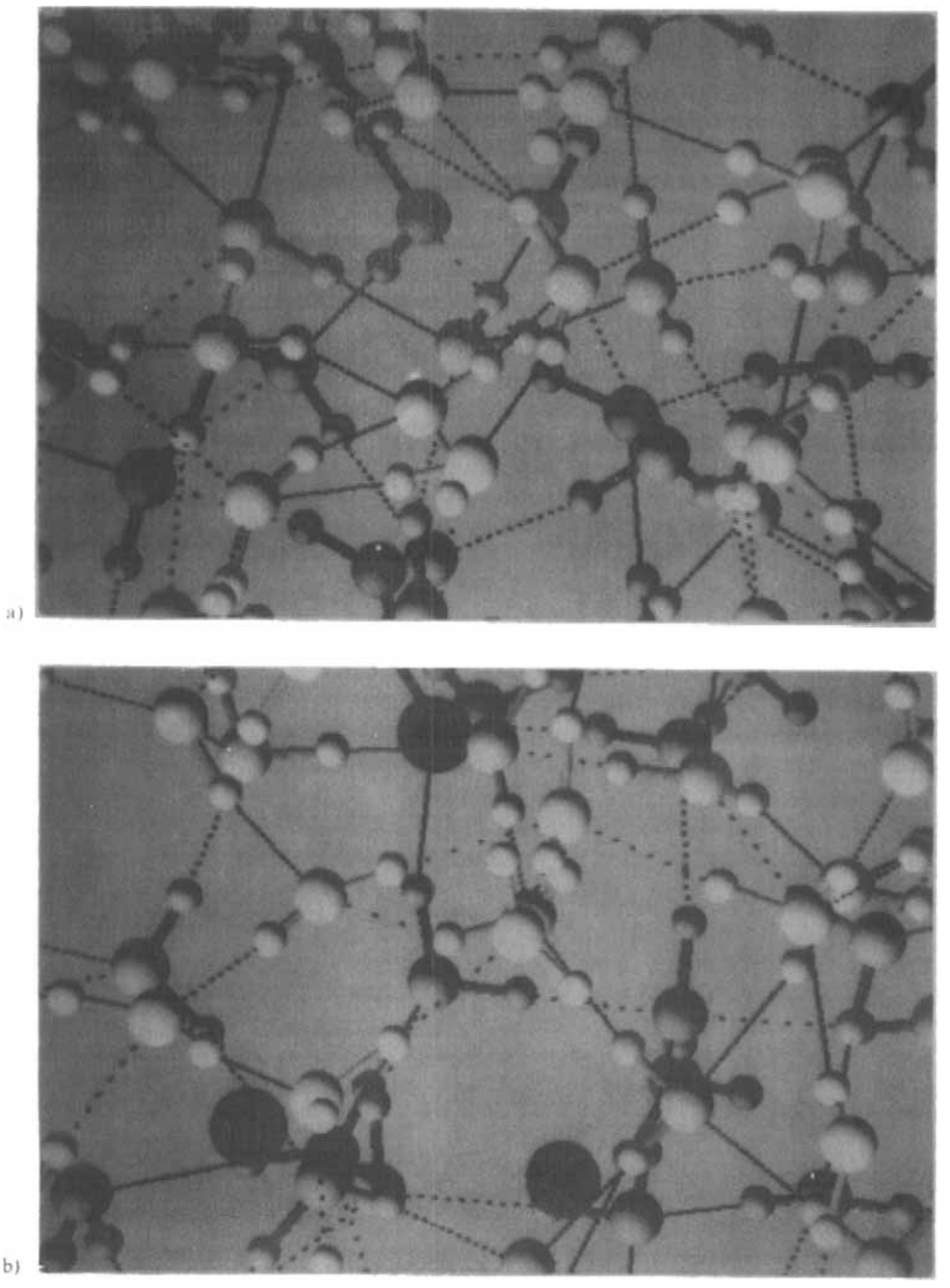

Figure 3 Examples of quenched configurations for pure water (a) and Xe solution (b). Large and small spheres denote oxygen and hydrogen atoms, respectively. Stick stands for molecular framework. Dotted lines show hydrogen bond betwen two water molecules. In (b) the spheres larger than the oxygen atoms are Xe and are not connected by any bond.

Table 5 Free energy of harmonic oscillators in pure water (W) and aqueous solutions of Ne, Nr, and Xe. All the units are in kJ/mol. Only pV term for gas is taken into account. S, G, and T are entropy, Gibbs free energy, and temperature of the system, respectively

system	W	Ne	Nr	Xe
G	−47.10	−46.15	−46.23	−46.48
ΔG^E		+11.1	+7.7	+4.4
$T\Delta S^E$	+4.2	+7.2	+2.6	

$$S'/k = \alpha \int [1-\ln(\beta\hbar\omega)]\ g(\omega)\, d\omega \tag{4}$$

where T is the temperature of the system, k is Boltzmann constant and $\hbar$ is Planck constant divided by 2π, β is the inverse of kT, U_q is the average potential energy in quenched structure and α is the average number of degrees of freedom per molecule. The calculated free energies shown in Table 5 (the pV term for condensed phase is neglected) agree only their sign with observed values. The entropy decreases experimentally observed in the hydration of these atoms could not be reproduced only by taking account of the change in mode frequencies. Following Stillinger and Weber [9], the free energy A for the system in canonical ensemble can be written based on quenched structure as

$$\begin{aligned} A/kT &= -\ln Q \\ &= -\ln \sum_j \exp(-\beta U_j) \int \exp(-\beta \Delta U_j)\, d\mathbf{r}d\mathbf{p} \end{aligned} \tag{5}$$

where the sum is taken over all distinct quenched configurations, Q is canonical partition function, $\mathbf{r}$ includes both center of mass and orientational coordinates, $\mathbf{p}$

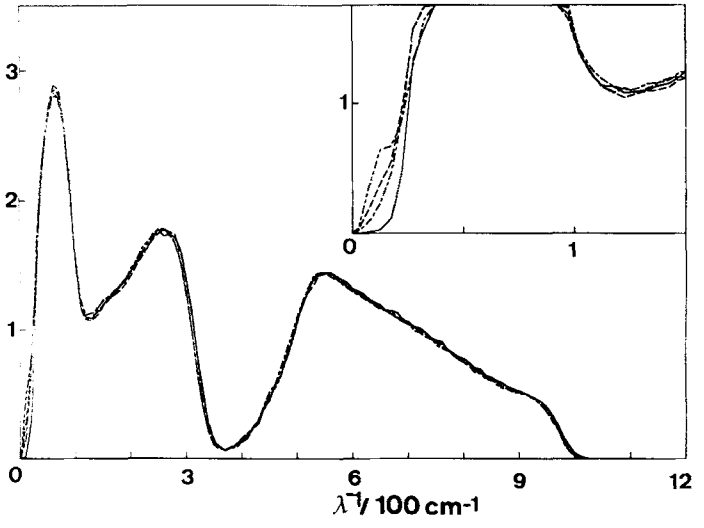

Figure 4 Density of State for pure water (solid line), Ne solution (dashed line), Nr solution (chain dotted line), and Xe (double chain dotted line). Detailed densities of states in the low frequency region are given in the inset.

stands for the associated conjugate momenta, and the integration spans each separated region by the quenching in configurational space. The free energy can be rewritten further as

$$A/kT = -\ln \int \exp [N(h(u) - \beta u - \beta f)]\, du \tag{6}$$

where N is the number of molecules in the system, u is potential energy per molecule, $h(u)$ is the density of distinct potential energy minima, f is vibrational free energy including an anharmonic contribution f_1 as well as a harmonic term f_0. For sufficiently large system, maximum term approximation can be applied. Thus A can be expressed as

$$A/kT = -N[h(u_m) - \beta u_m - \beta (f_0 + f_1)], \tag{7}$$

where u_m stands for potential energy value per particle at which the above integrand takes maximum.

In the free energy and entropy calculation within a harmonic approximation, only f_0 and u_m are taken into account. Therefore, the entropy of the system evaluated from f_0 and u_m does not agree with the experimental value [2]. The significant factors for negative entropy change are apparently $h(u_m)$, the number of distinct potential minimum configurations and f_1, the anharmonic term involved in vibrational free energy. Although it is very difficult to distinguish which effect is more important based only on the argument in this section, the relative magnitudes for various solute species can be discussed by the scrutiny of potentail energy difference in MD generated and quenched structures as shown above. It is plausible that the anharmonic term, which is important in liquid water to flatten the multi-dimensional surfaces, becomes less dominant with the existence of hydrophobic solutes.

IV. CONCLUDING REMARKS

Several molecular dynamics simulations have been carried out in order to investigate the hydrophobic hydration probed by Ne and Xe. The Ne solution with an ordinary size parameter failed to reproduce the observed thermodynamic quantities. It becomes possible to recover the exothermic hydration by only slightly enlarging the size parameter. The Xe solution with an ordinary size parameter can lead to exothermic hydration at infinite dilution. The size parameter difference in Ne and Nr is small. However, the structural feature in RDFs is qualitatively different to each other if we pay attention to quenched structures. The structural difference appears not only in the height of the peak but the location of the peak in the oxygen-oxygen RDF when a comparison of pure water is made with Nr (or Xe) solution: the shift to longer distance in the first peaks of oxygen-oxygen RDFs for solutions compared with that of pure water. These shifts are, in turn, caused by the increase in cyclic pentamer.

The size of apolar solute influences the density of state of intermolecular vibration. The density of state in Xe solution shifts to fairly lower frequency. However, the chemical potential of the Xe gas approximated as ideal one is also lower. This results in almost no free energy change in Xe solution. The entropies evaluated by imposing harmonic oscillator approximation does not agree well with experiment. This leads to consideration of other important factors which cause the entropy decrease in the hydration of apolar solutes. The harmonic approximation therefore partially elucida-

tes the observed thermodynamic quantities. The anharmonic contribution on the vibrational free energy seems to be decreased in the Ne solution as compared to pure water, where the anharmonic term is much larger than in the case of simple liquids. This observation is not seen in the Xe solution where the harmonic term is as large as in pure water. Further calculations on structures and free energies are underway.

Acknowledgement

The authors thank Mr. M. Matsumoto for providing a graphic display program. One of the authors (H.T.) is grateful to Prof. I. Ohmine and Dr. M. Sassai for stimulating discussions and providing a program for the ring analysis. Most of the calculations have been done in the Computer Centre of the Institute for Molecular Science and the Data Processing Centre of Kyoto University. This work is partially supported by the Grants in Aid for Scientific Research from the Ministry of Education in Japan.

References

[1] D. Eisenberg and W. Kauzmann "The Structure and Properties of Water", Oxford University Press, London (1969).
[2] F. Franks, "Water, A Comprehensive Treatise" ed. F. Franks, Vol. 2, Plenum, New York (1972).
[3] L.R. Pratt and D. Chandler, "Theory of the hydrophobic effect", *J. Chem. Phys.*, **67,** 3683 (1977).
[4] W. Swope and H.C. Andersen, "A molecular dynamics method for calculating the solubility of gases in liquids and the hydrophobic hydration of inert-gas atoms in aqueous solution", *J. Phys. Chem.*, **88,** 6548 (1984).
[5] A. Tani, "Solute-solute potential of mean force for non-polar molecules in water", *Mol. Phys.*, **51,** 161 (1983).
[6] H. Tanaka, "Integral equation and Monte Carlo study on hydrophobic effects", *J. Chem. Phys.*, **86,** 1512 (1987).
[7] L.R. Pratt, "Theory of hydrophobic effects", *An. Rev. Phys. Chem.*, **36,** 433 (1985).
[8] F.H. Stillinger and T.A. Weber, "Dynamics of structural transitions in liquids", *Phys. Rev.* **A25,** 978 (1982).
[9] F.H. Stillinger and T.A. Weber, "Inherent structure in water", *J. Phys. Chem.* **87,** 2833 (1983).
[10] I. Ohimine, H. Tanaka, and P.G. Wolynes, "Large local energy fluctuations in water", **89,** 5852 (1988), H. Tanaka and I. Ohmine, "Potential energy surfaces for water dynamics", *J. Chem. Phys.*, **91,** 6318 (1989).
[11] W.L. Jorgensen, J. Chandrasekhar, J.D. Madura, R.W. Impey, and M.L. Klein, "Comparison of simple potential functions for simulating liquid water", *J. Chem. Phys.*, **79,** 926 (1983).
[12] H.E. Alper and R.M. Levy, "Computer simulations of the dielectric properties of water", *J. Chem. Phys.*, **91,** 1242 (1989).
[13] J.O. Hirschfelder, C.F. Curtiss, and R.B. Bird, "Molecular Theory of Gases and liquids" Wiley, New York (1954).
[14] H. Goldstein, "Classical Mechanics", Addison-Wesley, Reading, Mass. (1981).
[15] A. Pohorille, L.R. Pratt, R.A. LaViolette, M.A. Wilson, and R.D. MacElroy, "Comparison of the structure of harmonic aqueous gases and liquid water", *J. Chem. Phys.*, **87,** 6070 (1987).
[16] Preliminary Monte Carlo simulations at infinite dilution show that the excess enthalpies of hydration for Ne, Nr, and Xe solutes are +9, −9, and −16 kJ/mol, respectively. In these Monte Carlo simulations, the potential models are the same as those in the MD simulation at 3 mol% and the difference is only the solute concentration.